Amphibia-Reptilia

Remote sensing and citizen science to characterize the ecological niche of an endemic and endangered Costa Rican poison frog

Marina Garrido-Priego[1, 2, 3,*], David Aaragonés[4], H. Christoph Liedtke[1], Andrew Whitworth[3, 5], Ivan Gomez-Mestre[1]

1 – Department of Ecology and Evolution, Estación Biológica de Doñana (CSIC), 41092 Sevilla, Spain

2 - Division of Behavioural Ecology, Institute of Ecology and Evolution, University of Bern, Bern, Switzerland

3 - Osa Conservation, Conservation Science Team, Washington, DC, 20005, USA

4 - Remote Sensing and GIS Laboratory (LAST-EBD), Estación Biológica de Doñana (CSIC), 41092 Sevilla, Spain

5 - Institute of Biodiversity, Animal Health and Comparative Medicine, College of Medical, Veterinary and Life Sciences, University of Glasgow, Glasgow, G12 8QQ, UK

*Corresponding author; e-mail: marina.garridopriego@unibe.ch

ORCID iDs: Garrido-Priego: 0000-0001-6666-7834; Aaragonés: 0000-0003-4989-9005; Liedtke: 0000-0002-6221-8043; Whitworth: 0000-0001-6197-996X; Gomez-Mestre: 0000-0003-0094-8195

Supplementary material

Figure S1. Distribution of the 67 occurrences used to model the ecological niche of *P. vittatus*. All occurrences are obscured within 3km^2 grid cells encompassing the hidden true location. The map is in scale 1:1,200,000 and Coordinate Reference System (CRS) WGS84.

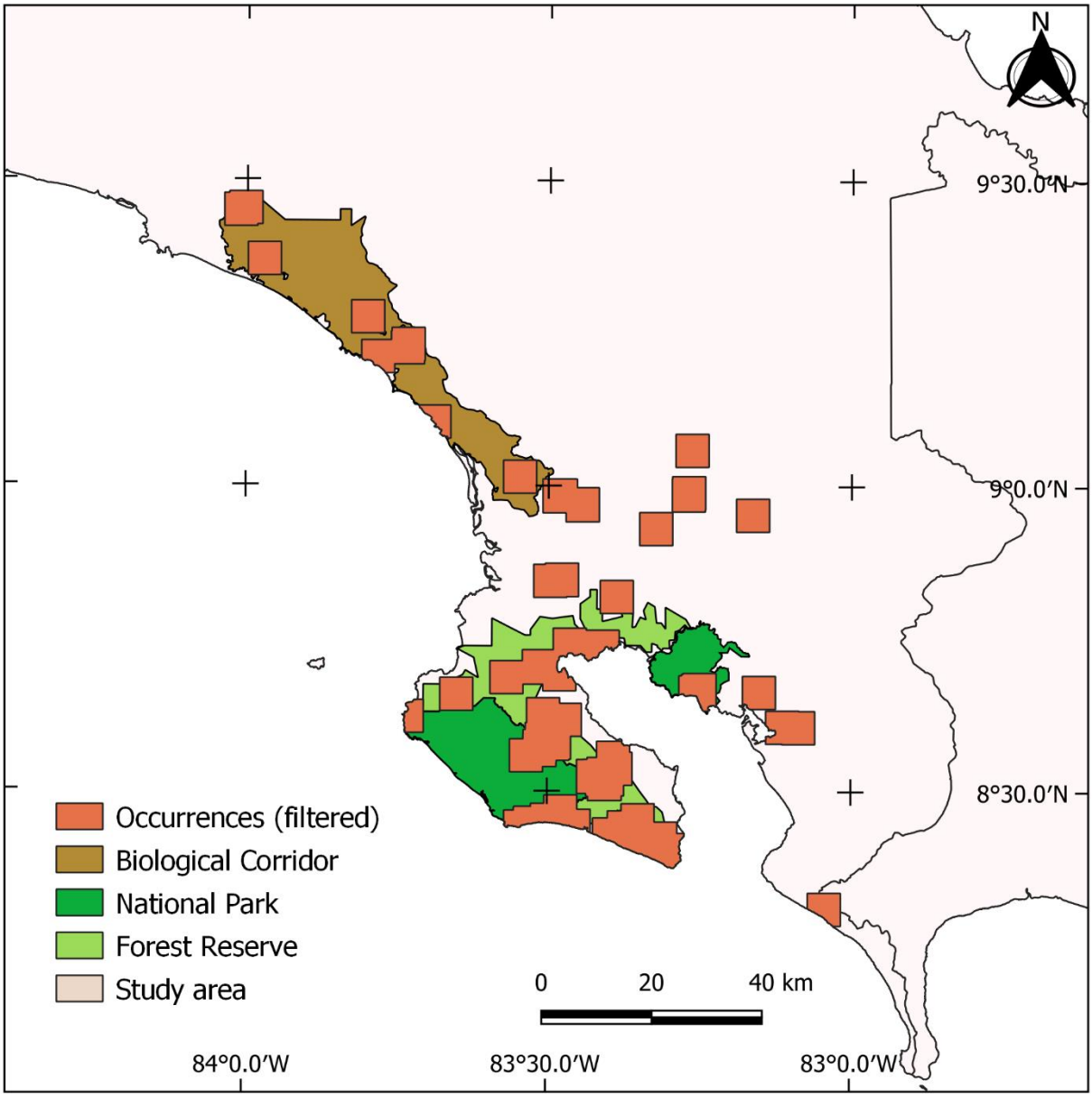

Text S1.

To get an up-to-date forest cover map of the study area, we mapped the land cover using Sentinel-2 satellite images processed in QGIS (3.10), working in UTM zone 17 north in World Geodesic System 1984 datum. Sentinel-2 offers a view of 13 bands in the visible, near infra-red and short-wave infra-red part of the electromagnetic spectrum, defined at 10 m, 20 m and 60 m of spatial resolution (Drusch et al., 2012). A graphic description of the steps taken below to obtain the land cover map can be seen in supplementary fig. S2.

To have a map with the smallest possible cloud cover, we acquired images from two dates during Costa Rica's dry season (2 March 2019 and 10 February 2019), previsualized in USGS Earth Explorer (https://earthexplorer.usgs.gov/). The distribution area of *P. vittatus* covers four different Sentinel-2 tiles: L16PKK, L17PKK, L16PKL, L17PKL; thus, we worked with these four tiles for both dates. We downloaded the 13 bands for each tile from Sentinels Scientific Data Hub (https://sci.hub.copernicus.eu/) using the Semi-Automatic Classification Plugin (SCP) for QGIS (Congedo, 2016). Sentinel-2 offers a wide variety of products depending on the image-processing levels. Level-1C gives information of the top of atmosphere reflectance. Level-2A is the atmospheric correction of Level-1C products, giving the surface reflectance as a result (Drusch et al., 2012; Louis et al., 2016). Thus, we downloaded band 10 on Level-1C to be able to detect cirrus (Baillarin et al., 2012). The rest of bands were downloaded on Level-2A.

Since most of Sentinel-2 bands are in 10x10 m spatial resolution (Drusch et al., 2012), this was the resolution used (Nivedita Priyadarshini et al., 2018). We also re-projected the tiles from zone 16 N to zone 17 N. Each band was set in a mosaic, setting together the four tiles (L16PKK projected to 17 N, L17PKK, L16PKL projected to 17 N and L17PKL) using SAGA (Conrad et al., 2015).

The four tiles cover an area larger than the total distribution range of *P. vittatus*, which was therefore comprised within the total study area. Hence, to simplify the analysis, we also applied a mask that encompassed all the area from the coastal line to the contour line of 1,500 m in altitude. We did not set the altitude limit at 550 m (see *P. vittatus* altitudinal range in species description) because we wanted to analyze whether there could be a potentially suitable area for *P. vittatus* at higher elevations, even if they may not have been occupied or explored by the species yet. Additionally, we also wanted to consider whether the suitable niche for *P. vittatus* would extend over the Panama side in the vicinity of the Costa Rican border. Therefore, we included in our study area the Panamanian area included within the tiles used (1,260.21 km^2). Then, using SCP (Congedo, 2016), the mosaics were stacked to create a raster band set for each date. Afterwards, using the software Idrisi, we obtained the radiometric normalization for both dates using 103 polygons in pseudo-invariant areas (Díaz-Delgado et al., 2016). The radiometric normalization allowed us to compare both images.

To remove the interference of clouds, we applied a cloud-mask for each date. To build these masks we used three bands: band 1, band 8 and band 10. we used band 1 to detect most of the clouds. Band 1 (centered at a 443 nm wavelength and called coastal/aerosol) is one of the bands in which is easier to identify clouds (Drusch et al., 2012). It is also important to consider clouds' shadow but, since it is difficult to differentiate them from water bodies, we considered them together. To do so, we used band 8 (centered at 865 nm wavelength, Near Infrared band) to distinguish clouds' shadows (Zhu et al., 2015). Lastly, we used band 10 (centered at 1380 nm wavelength and called the cirrus band) to identify high altitude clouds (Van der Meer et al., 2014).

To differentiate vegetation from other land cover types of the study area, we calculated the Normalized Difference Vegetation Index (NDVI) from the images using the NDVI ratio for Sentinel-2: NDVI = (B8 – B4) / (B8 + B4) (Tucker, 1979). The NDVI is extensively used to

analyze the vegetation cover, allowing us to distinguish between vegetated and not vegetated areas, and even among vegetation types (Wang et al., 2004). Pixels with negative values or close to zero corresponded to non-vegetated areas: water surfaces, urban areas, bare ground and clouds. Pixels with values close to 1 corresponded to dense vegetation. We masked the non-dense vegetated areas with values under 0.7 since we wanted to make sure we were then obtaining dense vegetation. This NDVI value of 0.7 is a recurrent value in tropical forests to detect forest areas, avoiding detecting shrublands (e.g., Arroyo-Mora et al., 2005; Baniya et al., 2018; Doughty and Goulden, 2009; Los et al., 2019; Martinuzzi et al., 2008). After applying the NDVI mask for both dates, we combined both images together, using the image from date 02/03/2019 as the main image since it had less cloud cover the image from 10/02/2019. We then filled out the masked clouds' area from 02/03/2019 with the 10/02/2019 image. This way cloud cover from date 02/03/2019 was reduced to a 2%. From this point, we kept working on this main image.

We performed an unsupervised 'k-means' classification (Likas et al., 2003) on this main image, clustering the pixels into 35 groups. Each cluster was inspected individually using photointerpretation with high-resolution Google Satellite orthophotos to determine the land cover type illustrated. Clusters that illustrated the same land cover type were grouped together, reclassifying these 35 clusters into 5 spectral classes. We post processed the classification using a sieve filter, which replaces cells' values based on the majority of the continuous neighboring cells. After the classification, we generated a mask for the dense crops (palm, white teak and pineapple) that were grouped together with forest clusters during the non-supervised classification using high-resolution Google Satellite orthophotos. Due to the difficulty in identifying white teak crops from orthophoto images, a few such plantations may not have been properly identified. Since the images used are from Costa Rica's dry season, the Corcovado lagoon was not at its full capacity and appeared as a mixture of pixels with diverse values. Thus,

we identified the area as 'wetland' using the Costa Rican digital atlas from 2014 (Ortiz-Malavasi, 2016). Finally, all the classes identified were reclassified into 9 categories using high-resolution Google Satellite orthophotos: Forest, tall/dense grassland, pasture, mangrove, palm plantation, pineapple plantation, white teak plantation, wetland and non-dense vegetated areas. Hence, obtaining the final product for the land cover map of the study area. We evaluated the land cover classification estimating accuracy and area from the sample data in an error matrix (supplementary text S1, table 1). We applied the proportional approaches sample allocations methodologies suggested by Olofsson et al. (2014), using the Cochran´s (1977) sample size formula for stratified random sampling. Using this final output, we calculated the percentage of forest over the study area. We then calculated the percentage of forest on every pixel of 1 km^2, in order to have every model predictor at the same resolution. To facilitate the analysis, we projected this predictor to geographical coordinates.

Table 1. Error matrix showing the estimated accuracy and area from the land cover classification. This error matrix was built using a total of 399 random points.

	1 (Teka)	2 (Pineapple)	3 (Palm)	4 (Lagoon)	5 (Pasture)	6 (Grassland)	7 (Forest)	8 (Mangrove)	9 (Others)	Total	User accuracy	Total class area (km²)
1	30	0	0	0	0	0	0	0	0	30	1	45.47
2	0	30	0	0	0	0	0	0	0	30	1	83.17
3	0	0	30	0	0	0	0	0	0	30	1	761.68
4	0	0	0	30	0	0	0	0	0	30	1	11.32
5	0	0	4	0	24	2	0	0	0	30	0,8	419.25
6	0	0	0	0	0	22	7	0	1	30	0,73333	1064.09

7	0	0	1	0	0	1	80	0	0	82	0,97561	3826.58
8	0	0	0	0	0	0	0	30	0	30	1	159.86
9	0	0	0	0	1	4	3	0	99	107	0,96104	3855.4
Total	30	30	35	30	25	29	90	30	100	399		10226.85
Producer accuracy	1	1	0,85714	1	0,96	0,75862	0,88889	1	0,74		0,87719	

References

Arroyo-Mora, J. P., Sánchez-Azofeifa, G. A., Kalacska, M. E. R., Rivard, B., Calvo-Alvarado, J. C., & Janzen, D. H. (2005). Secondary forest detection in a neotropical dry forest landscape using Landsat 7 ETM+ and IKONOS imagery. *Biotropica*, *37*(4), 497–507. https://doi.org/10.1111/j.1744-7429.2005.00068.x

Baillarin, S. J., Meygret, A., Dechoz, C., Petrucci, B., Lacherade, S., Tremas, T., Isola, C., Martimort, P., & Spoto, F. (2012). Sentinel-2 level1 products and image processing performances. *IGARSS*, 7003–7006.

Baniya, B., Tang, Q., Huang, Z., Sun, S., & Techato, K. anan. (2018). Spatial and temporal variation of NDVI in response to climate change and the implication for carbon dynamics in Nepal. *Forests*, *9*(6), 1–18. https://doi.org/10.3390/f9060329

Congedo, L. (2016). *Semi-Automatic Classification Plugin*. https://doi.org/http://dx.doi.org/10.13140/RG.2.2.29474.02242/1

Conrad, O., Bechtel, B., Bock, M., Dietrich, H., Fischer, E., Gerlitz, L., Wehberg, J., Wichmann, V., & Böhner, J. (2015). System for Automated Geoscientific Analyses (SAGA) v. 2.1.4. *Geoscientific Model Development*, *8*(7), 1991–2007. https://doi.org/10.5194/gmd-8-1991-2015

Díaz-Delgado, R., Aragonés, D., Afán, I., & Bustamante, J. (2016). Long-term monitoring of the flooding regime and hydroperiod of Doñana marshes with landsat time series (1974-2014). *Remote Sensing*, *8*(9), 1–19. https://doi.org/10.3390/rs8090775

Doughty, C. E., & Goulden, M. L. (2009). Seasonal patterns of tropical forest leaf area index and CO2 exchange. *Journal of Geophysical Research: Biogeosciences*, *114*(1), 1–12. https://doi.org/10.1029/2007JG000590

Drusch, M., Del Bello, U., Carlier, S., Colin, O., Fernandez, V., Gascon, F., Hoersch, B., Isola, C., Laberinti, P., Martimort, P., Meygret, A., Spoto, F., Sy, O., Marchese, F., & Bargellini, P. (2012). Sentinel-2: ESA's Optical High-Resolution Mission for GMES Operational Services. *Remote Sensing of Environment*, *120*, 25–36. https://doi.org/10.1016/j.rse.2011.11.026

Likas, A., Vlassis, N., & J. Verbeek, J. (2003). The global k-means clustering algorithm. *Pattern Recognition*, *36*(2), 451–461. https://doi.org/10.1016/S0031-3203(02)00060-2

Los, S. O., Street-Perrott, F. A., Loader, N. J., Froyd, C. A., Cuní-Sanchez, A., & Marchant, R. A. (2019). Sensitivity of a tropical montane cloud forest to climate change, present, past and future: Mt. Marsabit, N. Kenya. *Quaternary Science Reviews*, *218*, 34–48. https://doi.org/10.1016/j.quascirev.2019.06.016

Louis, J., Debaecker, V., Pflug, B., Main-Knorn, M., Bieniarz, J., Mueller-Wilm, U., Cadau, E., & Gascon, F. (2016). Sentinel-2 SEN2COR: L2A processor for users. *European Space Agency, (Special Publication) ESA SP*, *SP-740*(May), 9–13.

Martinuzzi, S., Gould, W. A., Ramos Gonzalez, O. M., Robles, A. M., Maldonado, P. C., Pérez-Buitrago, N., & Fumero Caban, J. J. (2008). Mapping tropical dry forest habitats integrating Landsat NDVI, Ikonos imagery, and topographic information in the Caribbean Island of Mona. *Revista de Biologia Tropical*, *56*(2), 625–639.

https://doi.org/10.15517/rbt.v56i2.5613

Nivedita Priyadarshini, K., Kumar, M., Rahaman, S. A., & Nitheshnirmal, S. (2018). a Comparative Study of Advanced Land Use/Land Cover Classification Algorithms Using Sentinel-2 Data. *The International Archives of the Photogrammetry, Remote Sensing and Spatial Information Sciences*, *XLII–5*(November), 665–670. https://doi.org/10.5194/isprs-archives-xlii-5-665-2018

Ortiz-Malavasi, E. (2016). Atlas de Costa Rica 2014. In *Repositorio del Tecnológico de Costa Rica*.

Tucker, C. J. (1979). Red and photographic infrared linear combinations for monitoring vegetation. *Remote Sensing of Environment*, *8*(2), 127–150. https://doi.org/10.1016/0034-4257(79)90013-0

Van der Meer, F. D., van der Werff, H. M. A., & van Ruitenbeek, F. J. A. (2014). Potential of ESA's Sentinel-2 for geological applications. *Remote Sensing of Environment*, *148*, 124–133. https://doi.org/10.1016/j.rse.2014.03.022

Wang, Q., Tenhunen, J., Dinh, N. Q., Reichstein, M., Vesala, T., & Keronen, P. (2004). Similarities in ground- and satellite-based NDVI time series and their relationship to physiological activity of a Scots pine forest in Finland. *Remote Sensing of Environment*, *93*(1–2), 225–237. https://doi.org/10.1016/j.rse.2004.07.006

Zhu, Z., Wang, S., & Woodcock, C. E. (2015). Improvement and expansion of the Fmask algorithm: Cloud, cloud shadow, and snow detection for Landsats 4-7, 8, and Sentinel 2 images. *Remote Sensing of Environment*, *159*, 269–277. https://doi.org/10.1016/j.rse.2014.12.014

Figure S2. Schematic representation of the land cover methodology followed.

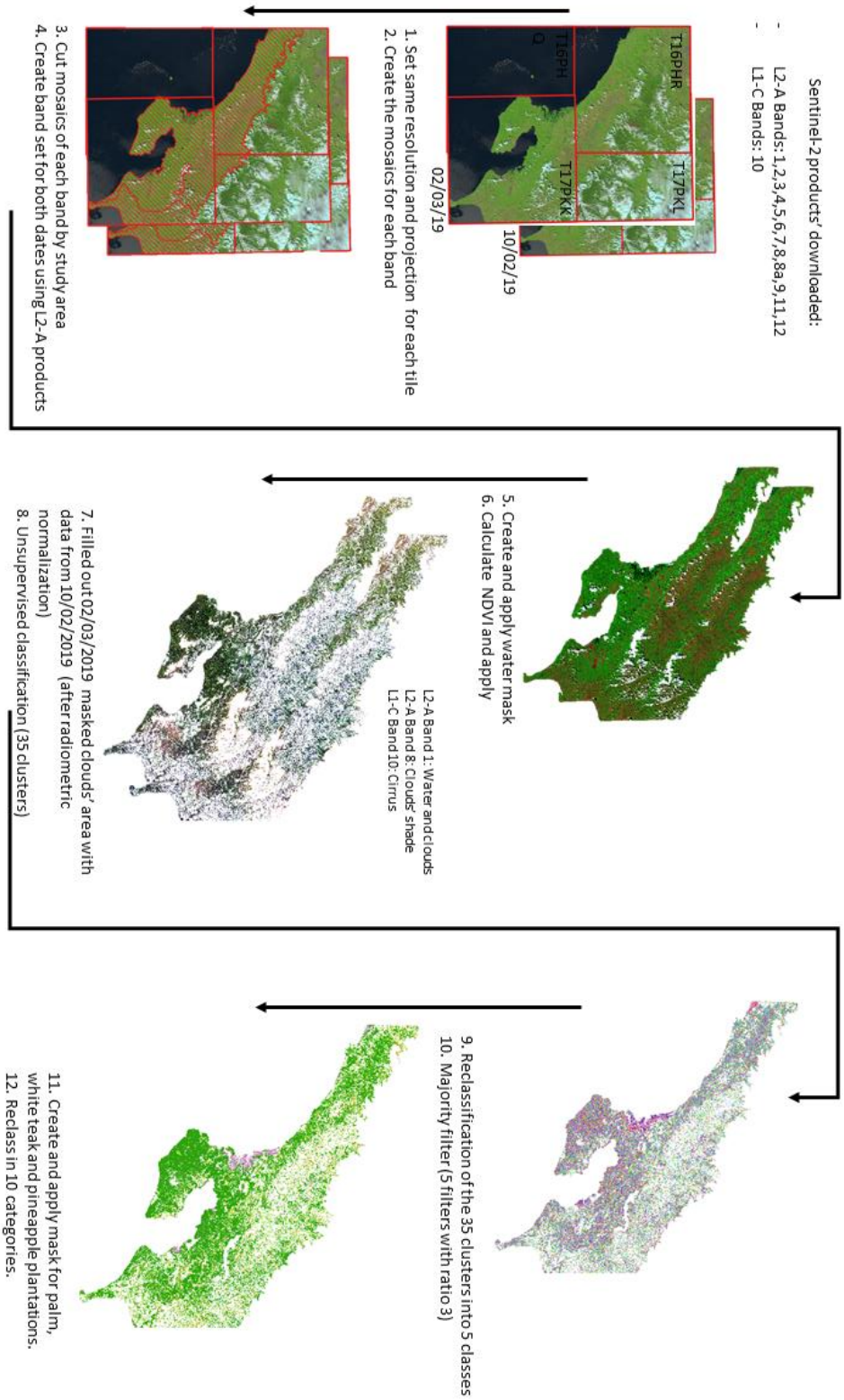

Table S1. Correlation matrix of all the variables studied: nineteen bioclimatic variables from WorldClim 2.1, distance to asadas, lakes and rivers, elevation, aspect, slope and forest percentage. In bold are the variables we used in the models.

Variables	Meaning	bio1	bio2	bio3	bio4	bio5	bio6	bio7
bio1	Annual Mean Temp.	1.000	-0.415	-0.544	0.831	0.974	0.985	-0.266
bio2	Mean Diurnal Range	-0.415	1.000	0.527	-0.446	-0.215	-0.556	0.942
bio3	Isothermality	-0.544	0.527	1.000	-0.717	-0.525	-0.557	0.211
bio4	Temp. Seasonality	0.831	-0.446	-0.717	1.000	0.811	0.823	-0.228
bio5	Max Temp. Warmest Month	0.974	-0.215	-0.525	0.811	1.000	0.924	-0.044
bio6	Min Temp. Coldest Month	0.985	-0.556	-0.557	0.823	0.924	1.000	-0.422
bio7	**Temp. Annual Range**	-0.266	0.942	0.211	-0.228	-0.044	-0.422	1.000
bio8	Mean Temp.Wettests Quarter	0.996	-0.395	-0.529	0.823	0.974	0.979	-0.249
bio9	Mean Temp. Driest Quarter	0.997	-0.425	-0.552	0.827	0.969	0.984	-0.274
bio10	Mean Temp. Warmest Quarter	1.000	-0.420	-0.558	0.843	0.974	0.985	-0.266
bio11	Mean Temp. Coldest Quarter	1.000	-0.411	-0.536	0.818	0.974	0.985	-0.265
bio12	Annual Precipitation	0.390	-0.345	-0.187	0.343	0.321	0.416	-0.325
bio13	Prep. Wettest Month	0.237	-0.318	-0.163	0.223	0.170	0.271	-0.303
bio14	Prep. Driest Month	0.175	-0.178	-0.232	0.200	0.150	0.180	-0.113
bio15	**Prep. Seasonality**	-0.061	-0.032	0.083	-0.021	-0.073	-0.040	-0.069
bio16	**Prep. Wettest Quarter**	0.322	-0.330	-0.150	0.302	0.254	0.354	-0.322
bio17	**Prep. Driest Quarter**	0.208	-0.201	-0.238	0.186	0.175	0.212	-0.139
bio18	**Prep. Warmest Quarter**	0.327	-0.193	-0.347	0.356	0.316	0.319	-0.085
bio19	**Prep.Coldest Quarter**	0.476	-0.444	-0.384	0.453	0.408	0.508	-0.359
D. Asadas	**Distance from Asadas**	0.203	-0.401	-0.233	0.135	0.126	0.257	-0.372
Aspect	**Aspect**	-0.071	0.037	0.068	-0.087	-0.071	-0.070	0.016
Elevation	**Elevation**	-0.884	0.448	0.452	-0.735	-0.836	-0.888	0.339
D. lakes	**Distance from lakes**	-0.191	-0.199	0.130	-0.278	-0.259	-0.128	-0.280
D. rivers	**Distance from rivers**	0.053	-0.389	-0.259	-0.012	-0.013	0.122	-0.350
Forest per.	**Forest percentage**	0.098	-0.109	0.043	0.054	0.055	0.104	-0.141
Slope	**Slope**	-0.281	0.148	0.210	-0.296	-0.273	-0.282	0.091

bio8	bio9	bio10	bio11	bio12	bio13	bio14	bio15	bio16	bio17	bio18	bio19
0.996	0.997	1.000	1.000	0.390	0.237	0.175	-0.061	0.322	0.208	0.327	0.476
-0.395	-0.425	-0.420	-0.411	-0.345	-0.318	-0.178	-0.032	-0.330	-0.201	-0.193	-0.444
-0.529	-0.552	-0.558	-0.536	-0.187	-0.163	-0.232	0.083	-0.150	-0.238	-0.347	-0.384
0.823	0.827	0.843	0.818	0.343	0.223	0.200	-0.021	0.302	0.186	0.356	0.453
0.974	0.969	0.974	0.974	0.321	0.170	0.150	-0.073	0.254	0.175	0.316	0.408
0.979	0.984	0.985	0.985	0.416	0.271	0.180	-0.040	0.354	0.212	0.319	0.508
-0.249	-0.274	-0.266	-0.265	-0.325	-0.303	-0.113	-0.069	-0.322	-0.139	-0.085	-0.359
1.000	0.992	0.996	0.996	0.368	0.217	0.161	-0.057	0.303	0.193	0.322	0.439
0.992	1.000	0.996	0.996	0.398	0.241	0.186	-0.073	0.325	0.222	0.322	0.493
0.996	0.996	1.000	0.999	0.389	0.237	0.177	-0.060	0.322	0.209	0.330	0.479
0.996	0.996	0.999	1.000	0.388	0.235	0.172	-0.062	0.319	0.207	0.323	0.474
0.368	0.398	0.389	0.388	1.000	0.703	0.462	-0.052	0.879	0.480	0.637	0.716
0.217	0.241	0.237	0.235	0.703	1.000	0.185	0.439	0.847	0.190	0.338	0.627
0.161	0.186	0.177	0.172	0.462	0.185	1.000	-0.490	0.251	0.760	0.359	0.338
-0.057	-0.073	-0.060	-0.062	-0.052	0.439	-0.490	1.000	0.359	-0.685	-0.164	-0.065
0.303	0.325	0.322	0.319	0.879	0.847	0.251	0.359	1.000	0.200	0.436	0.629
0.193	0.222	0.209	0.207	0.480	0.190	0.760	-0.685	0.200	1.000	0.393	0.396
0.322	0.322	0.330	0.323	0.637	0.338	0.359	-0.164	0.436	0.393	1.000	0.365
0.439	0.493	0.479	0.474	0.716	0.627	0.338	-0.065	0.629	0.396	0.365	1.000
0.197	0.209	0.203	0.206	0.092	0.168	0.030	0.049	0.125	0.087	0.005	0.173
-0.071	-0.069	-0.072	-0.070	-0.012	-0.035	0.001	-0.053	-0.036	0.006	-0.040	-0.015
-0.882	-0.879	-0.884	-0.884	-0.396	-0.269	-0.158	0.015	-0.344	-0.187	-0.299	-0.406
-0.194	-0.179	-0.193	-0.183	-0.118	0.001	-0.112	0.071	-0.062	-0.064	-0.254	-0.017
0.047	0.068	0.053	0.057	-0.035	0.006	0.024	0.007	-0.027	0.028	-0.048	0.057
0.089	0.101	0.096	0.098	0.144	0.117	0.099	-0.176	0.066	0.201	0.062	0.254
-0.280	-0.277	-0.282	-0.277	-0.135	-0.090	-0.067	-0.070	-0.146	-0.008	-0.133	-0.080

D. Asadas	Aspect	Elevation	D. lakes	D. rivers	Forest per.	Slope
0.203	-0.071	-0.884	-0.191	0.053	0.098	-0.281
-0.401	0.037	0.448	-0.199	-0.389	-0.109	0.148
-0.233	0.068	0.452	0.130	-0.259	0.043	0.210
0.135	-0.087	-0.735	-0.278	-0.012	0.054	-0.296
0.126	-0.071	-0.836	-0.259	-0.013	0.055	-0.273
0.257	-0.070	-0.888	-0.128	0.122	0.104	-0.282
-0.372	0.016	0.339	-0.280	-0.350	-0.141	0.091
0.197	-0.071	-0.882	-0.194	0.047	0.089	-0.280
0.209	-0.069	-0.879	-0.179	0.068	0.101	-0.277
0.203	-0.072	-0.884	-0.193	0.053	0.096	-0.282
0.206	-0.070	-0.884	-0.183	0.057	0.098	-0.277
0.092	-0.012	-0.396	-0.118	-0.035	0.144	-0.135
0.168	-0.035	-0.269	0.001	0.006	0.117	-0.090
0.030	0.001	-0.158	-0.112	0.024	0.099	-0.067
0.049	-0.053	0.015	0.071	0.007	-0.176	-0.070
0.125	-0.036	-0.344	-0.062	-0.027	0.066	-0.146
0.087	0.006	-0.187	-0.064	0.028	0.201	-0.008
0.005	-0.040	-0.299	-0.254	-0.048	0.062	-0.133
0.173	-0.015	-0.406	-0.017	0.057	0.254	-0.080
1.000	-0.008	-0.220	0.238	0.473	0.160	-0.102
-0.008	1.000	0.077	0.032	-0.010	0.041	0.072
-0.220	0.077	1.000	0.132	-0.052	-0.067	0.306
0.238	0.032	0.132	1.000	0.141	0.015	0.150
0.473	-0.010	-0.052	0.141	1.000	-0.181	-0.110
0.160	0.041	-0.067	0.015	-0.181	1.000	0.222
-0.102	0.072	0.306	0.150	-0.110	0.222	1.000

Table S2. AICc and AUC values for the MaxEnt models built to analyse the ecological niche of *Phyllobates vittatus* in Costa Rica using occurrences collected between 2016 and 2020 and abiotic variables created and obtained in 2020.

Extent	Regularization multiplier	Feature class	AICc value	delta AICc	AUC train	AUC test
5 km buffer area	3	Q	1124.87	0	0.73	0.68
10 km buffer area	3	LQ	11205.51	0	0.79	0.76
Total extent area	3	LQ	1088.84	0	0.88	0.87

Table S3. Contribution to the characterization of the ecological niche of *Phyllobates vittatus* in Costa Rica from the MaxEnt model built using occurrences collected between 2016 and 2020 and abiotic variables created and obtained in 2020.

Variable	Meaning	Contribution (%)
Elevation	Elevation	57.5
Distance from lakes	Distance from lakes	13.7
Forest percentage	Forest percentage	13.4
Bio 7	Temp. annual range	6.9
Bio 15	Prep. Seasonality	3.9
Bio 19	Prep. Coldest Quarter	2.4
Bio 18	Prep. Warmest Quarter	0.9
Slope	Slope	0.7
Distance from rivers	Distance from rivers	0.5
Bio 16	Prep. Wettest Quarter	0
Bio 17	Prep. Driest Quarter	0
Aspect	Aspect	0
Distance from Asadas	Distance from Asadas	0

Figure S3. Distribution of the four main abiotic factors (i.e., altitude, distance to lakes, forest percentage and annual temperature range) that determine the ecological niche of *Phyllobates vittatus* in Costa Rica. All these maps are in scale 1:1,150,000 and CRS WGS 84.

A. Elevation

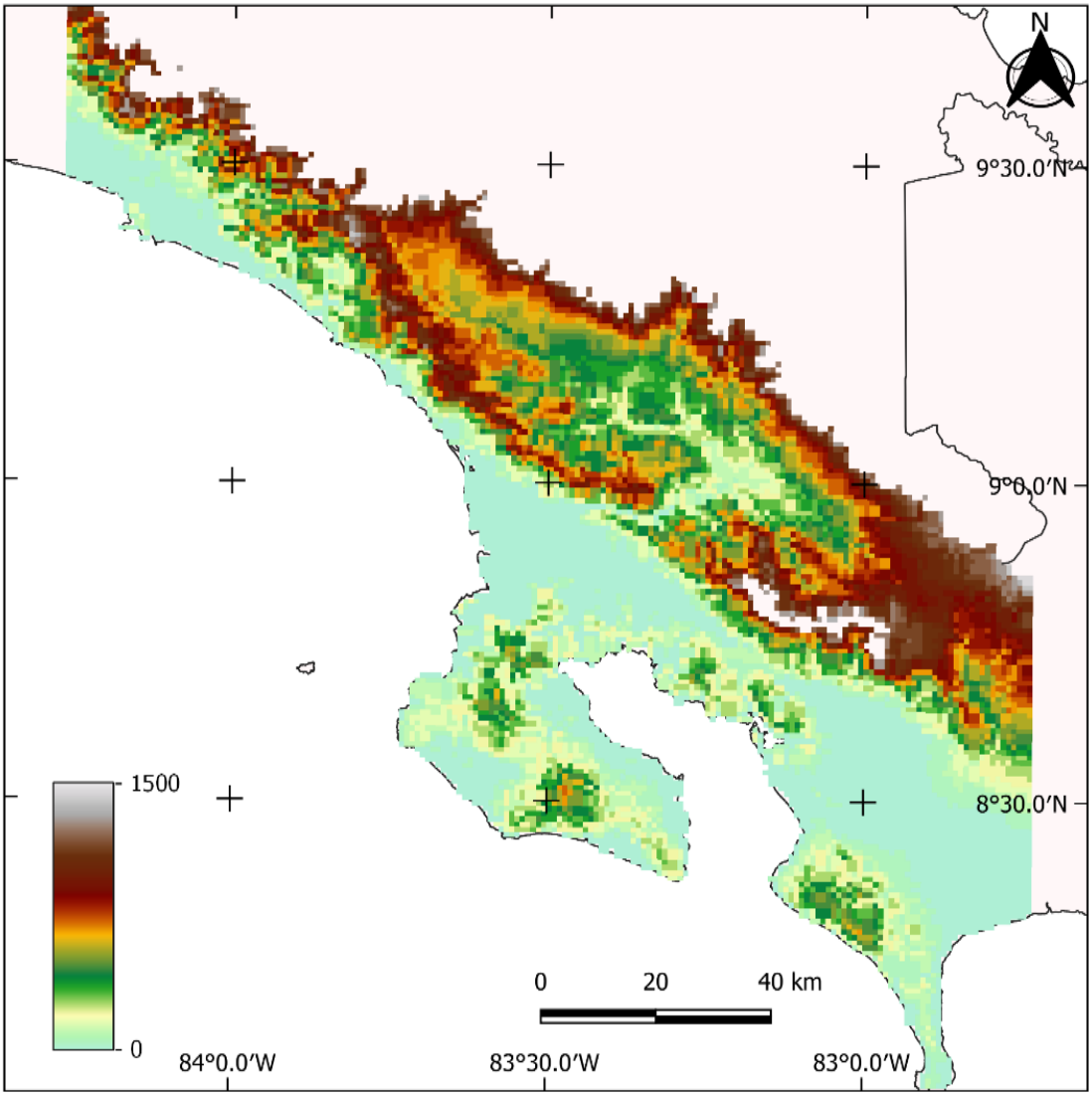

B. Distance to lakes

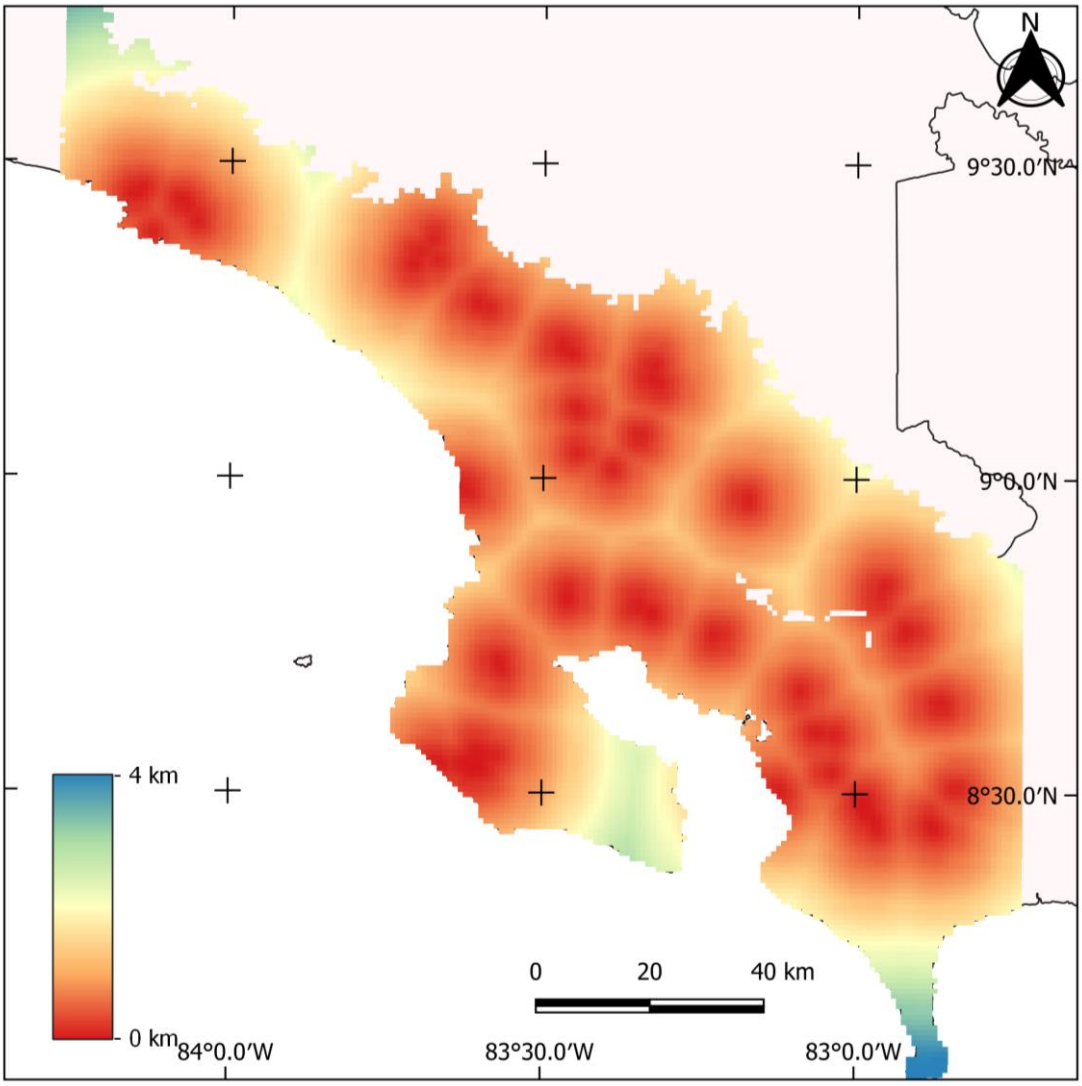

C. Forest percentage

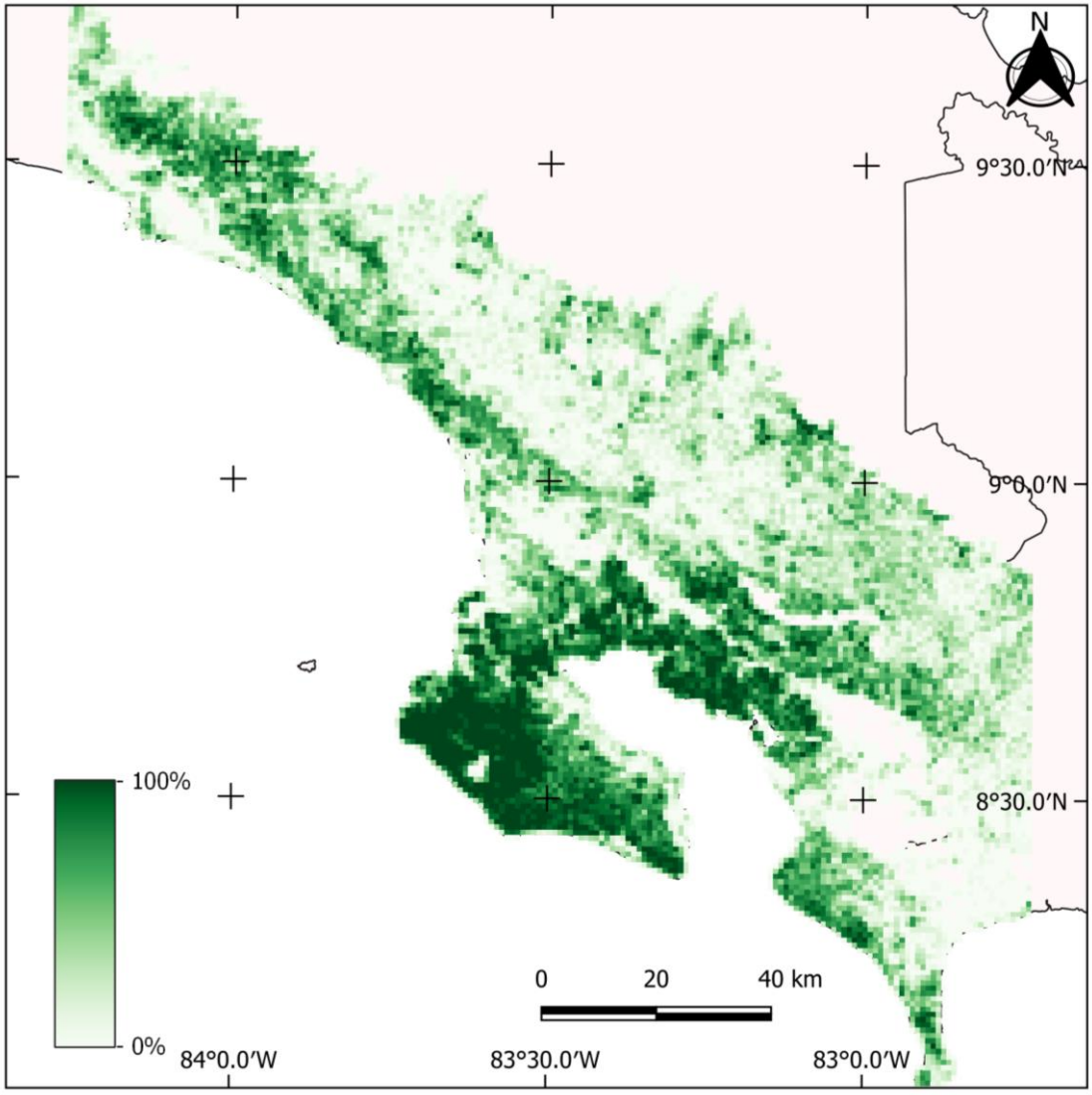

D. Annual temperature range

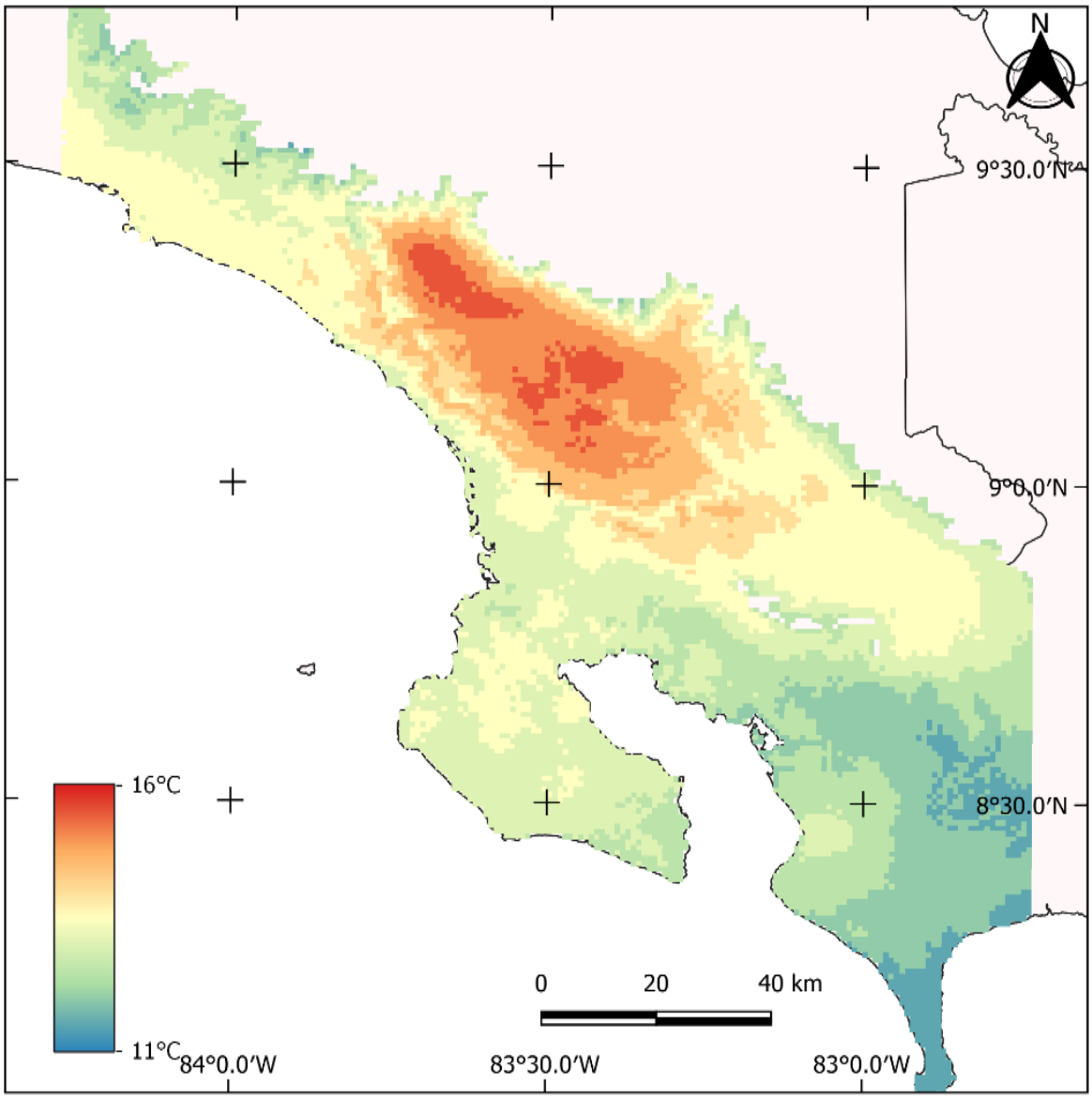

Figure S4. Response curves of species altitude, distance to lakes, distance to rivers, forest percentage and annual temperature range.

A. Elevation

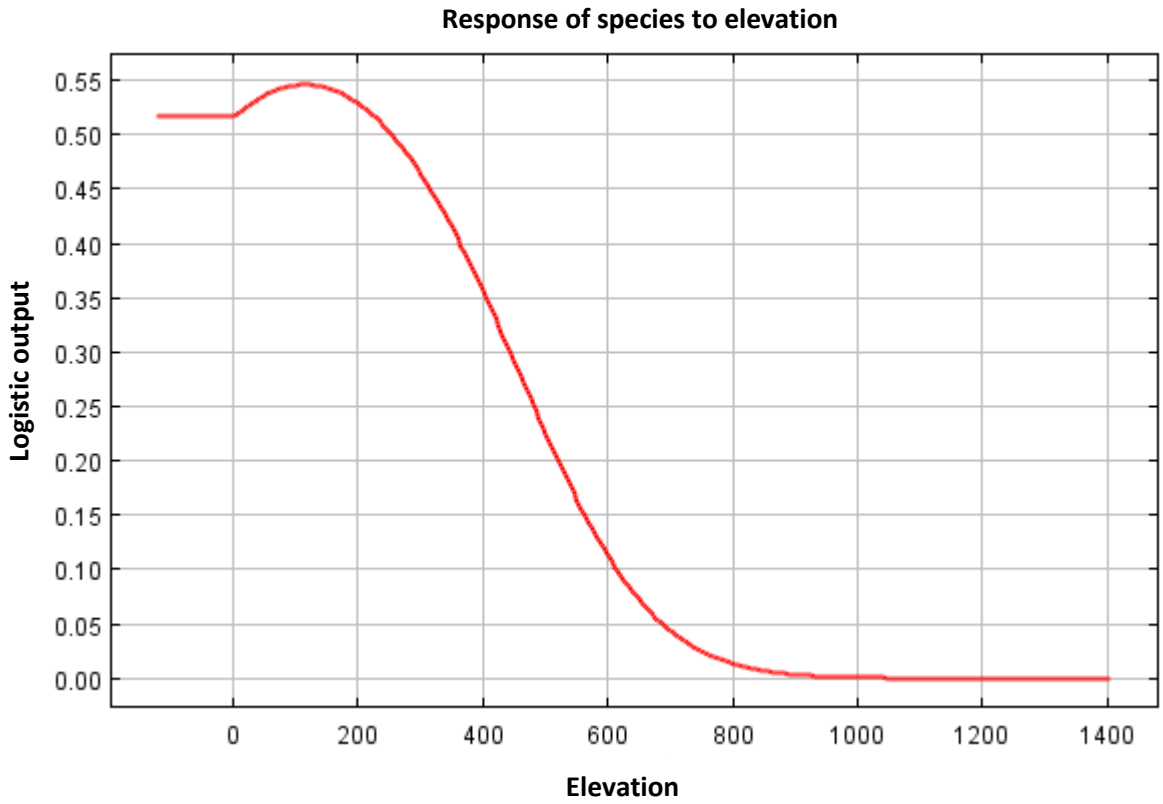

B. Distance to lakes

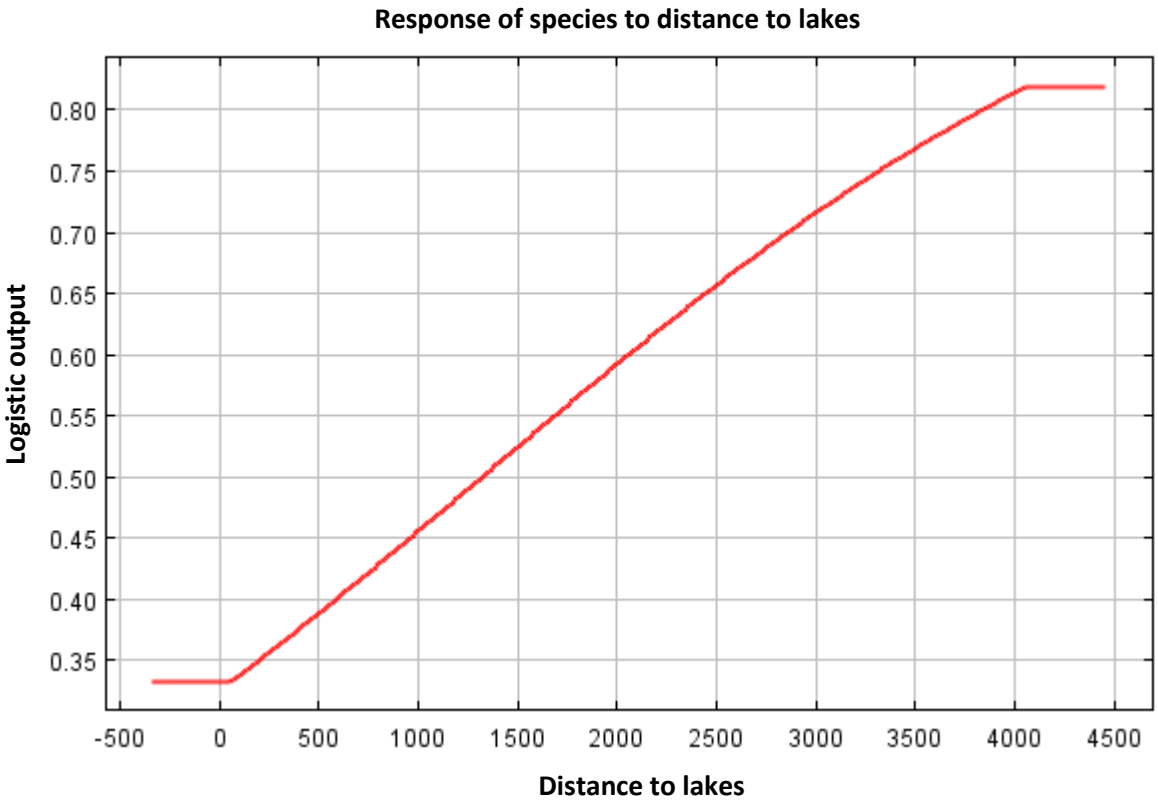

C. Distance to rivers

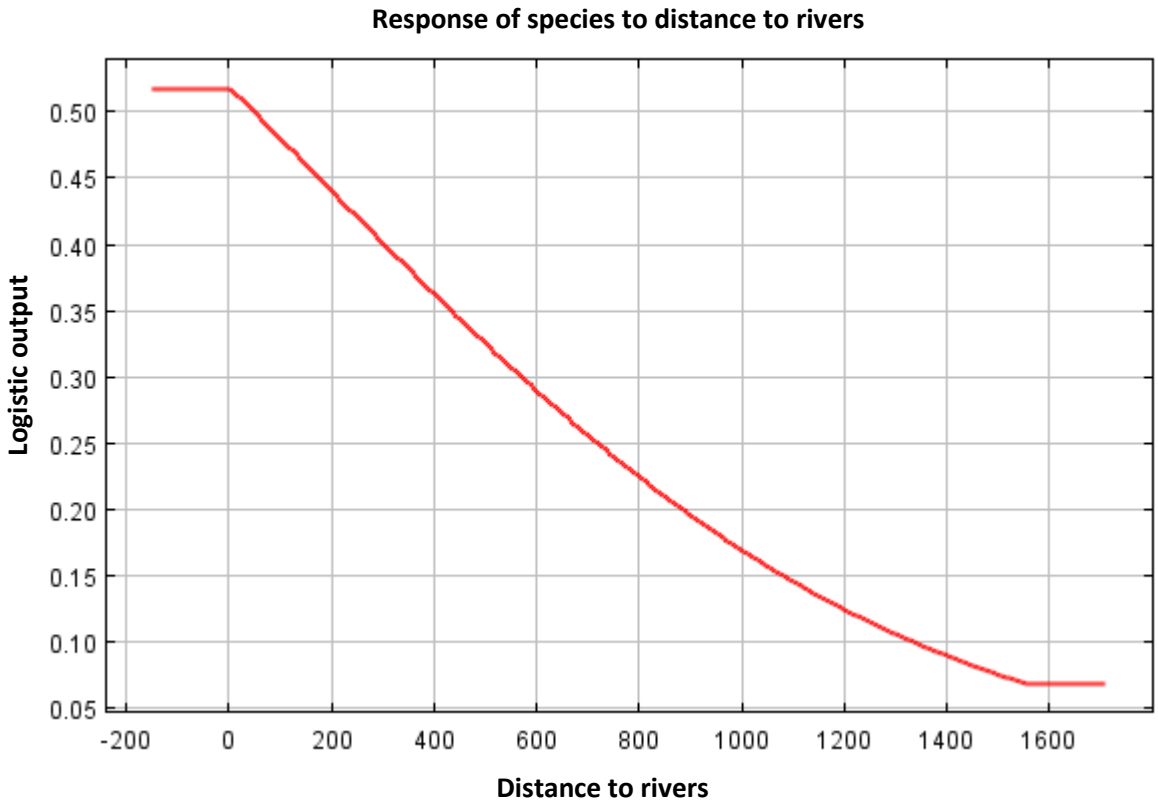

D. Forest percentage

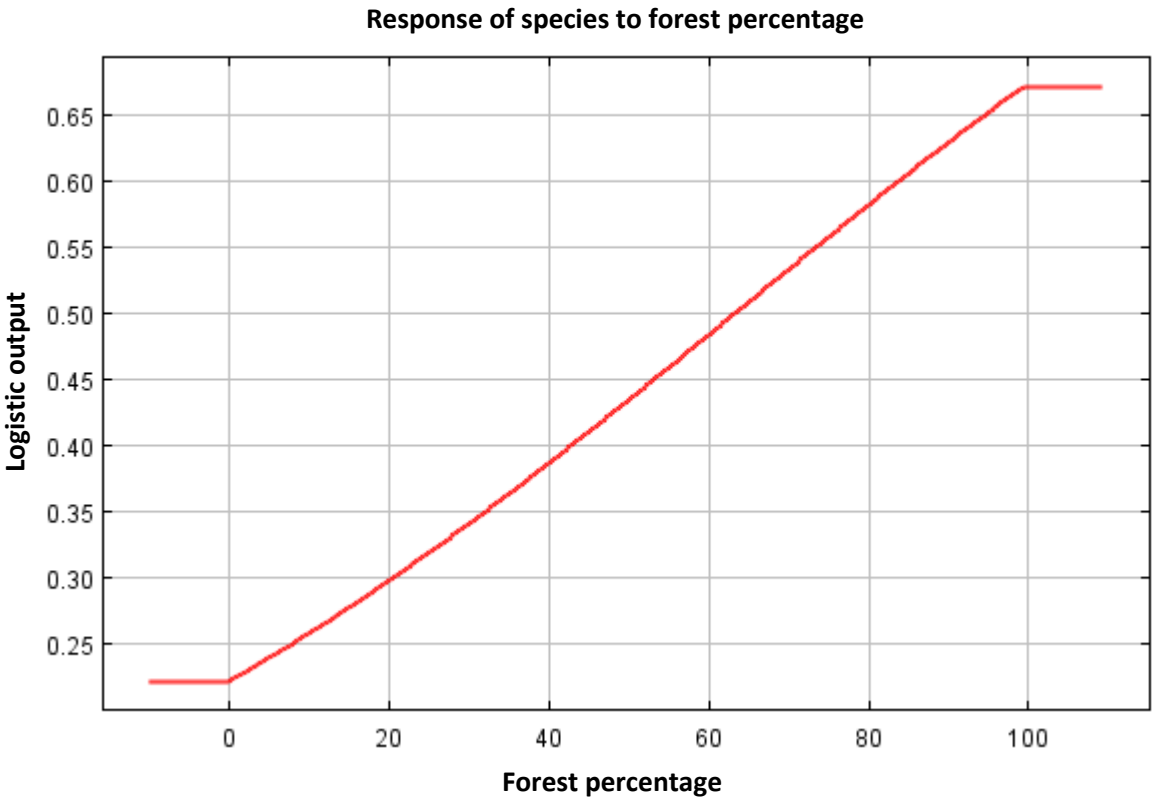

E. Annual temperature range (bio 7)